Self and Foreign Peptides Interact with Intact and Disassembled MHC Class II Antigen HLA-DR via Tryptophan Pockets†

Harald Kropshofer, Ines Bohlinger, Heiner Max, and Hubert Kalbacher*,‡

Medizinisch-naturwissenschaftliches Forschungszentrum, Universität Tübingen, Ob dem Himmelreich 7, D-7400 Tübingen, FRG

Received April 12, 1991; Revised Manuscript Received June 18, 1991

ABSTRACT: The acid release of endogenous peptides from immunoaffinity-pure human major histocompatibility complex (MHC) class II proteins HLA-DR1 is accompanied by an 18% decrease in intrinsic tryptophan fluorescence. The effect is totally reversible upon readdition of an autologous endogenous peptide fraction. High-performance size-exclusion chromatographic (HPSEC) binding and release studies with a nonfluorescent HLA-DR1-restricted influenza matrix peptide IM(18–29) prove the fact that Trp residues of the HLA protein change their fluorescence intensities. Since the far-UV circular dichroism spectra of HLA molecules before and after peptide release, DR1[NAT] and DR1[REL], show very small differences, we can rule out the breakdown of secondary structural elements under release conditions, although DR[REL] consists of diassembled α- and β-subunits, as evidenced by HPSEC. Quenching of DR1[NAT] and DR1[REL] using the neutral quencher acrylamide results in a 20% increase in total accessibility of the nine-residue Trp population whereas quenching by iodide yields only a 5% increase. Both results taken together tell us that two Trp residues, preferentially ones located in apolar pockets, become accessible upon the release of peptides. The significantly smaller fluorescence enhancement upon binding IM(18–29) of DR3[REL], exclusively lacking Trp-9(β_1), and the missing tendency to reassemble under the influence of IM(18–29) compared to DR1[REL] suggest an important role for position 9(β_1). The region around Trp-43(α_1) should be responsible for the binding of IM(18–29) to the α-subunits of DR1 and DR3, respectively, as verified by fluorometric HPSEC and SDS–PAGE. Obviously, our findings are in total agreement with the hypothetical MHC class II model, whereafter Trp-9(β_1) and Trp-43(α_1) besides Trp-61(β_1) are constituents of the binding groove of DR1. Extending the homology to MHC class I products, we postulate the existence of three hydrophobic pockets in the binding site of DR1 with the cited Trp residues being juxtaposed to contacting apolar peptide side chains in HLA–peptide complexes. According to the deduced two-residue-contact model the minimal consensus motif for DR1-restricted peptide antigens consists of two hydrophobic residues lying 14–16 Å apart in the bound state of the peptide.

The association of major histocompatibility complex (MHC)[1] molecules and peptidal forms of foreign antigens is a basic immunologic step (Townsend et al., 1986; Buus et al., 1986a). It is this bimolecular complex on the cell surface of antigen-presenting cells (APC) that normally is recognized by mature T cells leading to the initiation of a cellular immune cascade (Benacerraf, 1978; Ziegler & Unanue, 1982; Townsend et al., 1985). As a rule, peptides arising from endogenously synthesized proteins are associated to MHC class I molecules and are presented to $CD8^+$ T cells, whereas peptides derived from exogenous antigens are MHC class II restricted and recognized by $CD4^+$ T cells (Braciale et al., 1987; Demotz et al., 1989; Sweetser et al., 1989), although there is growing evidence that exceptions to this generalization do exist (Nuchtern et al., 1990; Chen et al., 1990). Peptide fragments of degraded self proteins cocrystallizing and copurifying with MHC molecules (Bjorkman et al., 1987; Buus et al., 1988; Wallny et al., 1990; Roetzschke et al., 1991) and binding studies with synthetic T-cell epitopes have shown us that MHC proteins are potent peptide receptors, in the absence of foreign antigens being constitutively associated to self peptides (Claverie & Kourilsky, 1986, Chen & Parham, 1989). Self peptide–MHC protein complexes are supposed to be decisively involved in induction and maintenance of tolerance as well as in being a target for alloreactive T-cell receptors (TCR) (Marrack & Kappler, 1988; Nikolic-Zugic & Bevan, 1990). Inside the cell, association with self peptides and targeting of class II MHC proteins depends on a 31-kDa protein, the invariant chain (Ii), as found by Roche and Cresswell (1990) and Lotteau et al. (1990). In contrast to the generally accepted view, that Ii prevents binding of endogenous peptides in the ER, Viguier et al. (1990) succeeded in isolating MHC–Ii–peptide complexes formed in vivo. Human leukocyte antigens DR (HLA-DR) are products of the human MHC class II and consist of the two noncovalently linked glycoprotein subunits α (34 kDa) and β (29 kDa) (Kaufmann & Strominger, 1979). HLA class II proteins can be modeled by using the far-reaching sequence homology to the X-ray crystallographically

† A preliminary account of this work was presented at the 10th International Symposium on HPLC of Proteins, Peptides, and Polynucleotides, October 29–31, 1990, Wiesbaden, FRG. The project was supported by the Sonderforschungsbereich 120.

* Correspondence should be sent to this author.

‡ The work done by H.K. was supported by a grant of the Deutsche Forschungsgemeinschaft.

[1] Abbreviations: MHC, major histocompatibility complex; HLA, human leukocyte antigen; Trp, tryptophan; EPF, endogenous peptide fraction; IM, influenza matrix peptide; Ig, immunoglobulin; TCR, T-cell receptor; HLA-DR[NAT], HLA-DR before peptide release; HLA-DR[REL], HLA-DR after peptide release, EBV, Epstein–Barr virus; CD, circular dichroism; HPLC high-performance liquid chromatography; HPSEC, high-performance size-exclusion chromatography; CHAPS, 3-[(3-cholamidopropyl)dimethylammonio]-1-propanesulfonate; DMF, *N*,*N*′-dimethylformamide; TFA, trifluoroacetic acid; SDS, sodium dodecyl sulfate; SDS–PAGE, sodium dodecyl sulfate–polyacrylamide gel electrophoresis; AMCA, 7-amino-4-methylcoumarin-3-acetic acid; ER, endoplasmic reticulum.

0006-2960/91/0430-9177$02.50/0

analyzed class I molecules HLA-A2 and HLA-Aw68 to adopt the following structure (Bjorkman et al., 1987): the N-terminal domains α_1 and β_1 of each subunit forming a pseudointermolecular dimer constitute the most prominent part of the molecule. This part is characterized by two long, lateral α-helices and an eight-stranded β-pleated sheet creating the base of a deep cleft (Brown et al., 1988). Polymorphic residues, which explain the peptide binding specifities of different HLA isotypes, accumulate significantly at positions that point into the groove (Kappes & Strominger, 1988). Similarities concerning the genomic organization and primary structure further suggest an Ig-like domain (α_2 or β_2), an α-helical transmembrane anchor, and a short cytosolic C-terminal domain in each subunit of class II HLA molecules, (Brown et al., 1988). The large cleft on the top surface of the heterodimer that is most easily accessible to TCRs is generally accepted to be the single peptide-binding site as evidenced by several observations: (i) successful peptide competition was performed on the cellular level (Guillet et al., 1986) and also with purified class II proteins (Guillet et al., 1987), (ii) cocrystallizing endogenous peptides of HLA-A2 and HLA-Aw68 obviously have remained bound during the entire isolation being consistent with the slow dissociation rate of class II HLA-restricted peptides (Buus et al., 1986b), and (iii) the dimensions of the site fit well with the length of synthetic peptides (5–20 residues) that are able to elicit T-cell responses (Rothbard & Taylor, 1988b; Van Bleek & Nathenson, 1990; Reddehase & Koszinowski, 1989).

SDS–PAGE analyses by Dornmair et al. (1989) led to the identification of two $\alpha\beta$ heterodimeric conformers ("compact" and "floppy"). Using the same technique, Dornmair et al. (1990) found that disassembled α- and β-chains as well as the α-chain of class I molecules deprived of β_2 microglobulin (Dornmair et al., 1991) are able to bind antigenic peptides specifically. Endogenous peptides could be released from the binding cleft of MHC class II proteins by acid treatment (Buus et al., 1988). Compositional analyses of the endogenous peptide fraction (EPF) of the mouse class II isotype I-A^d revealed a high molecular mass diversity ($\leq$10 kDa) (Buus et al., 1988). This indicates that class II associated peptides have variable length.

In a comparison of the fine structure of the class I products HLA-A2 and HLA-Aw68, Garrett et al. (1989) describe several allele-specific subsites in the peptide-binding groove, called "specifity pockets". The chemical character of the latter is altered by blockwise exchange of polymorphic residues. Since a most recent study of Peccoud et al. (1990) shows perfect homology between HLA class I and II molecules, as concerns the location of antigen contact residues belonging to the helix of the α_1-domain, we wondered whether the pocket hypothesis also holds for HLA-DR proteins.

In the present work we make use of a new highly sensitive method, recently introduced by Kalbacher and Kropshofer (1991), to detect interactions between peptides and MHC proteins, exploiting the fact that class II–peptide complexes are sufficiently stable to be separated by gel filtration techniques (Buus et al., 1986a). We point out that structural changes of HLA-DR molecules upon release of in vivo bound endogenous peptides and, conversely, upon binding of antigenic peptides in vitro can be characterized physicochemically by noninvasive fluorescence assays. With class I related homologies in sequence and structure revealing that the only fluorescent Trp residues in the peptide-binding domains α_1 and β_1 are located in analogous pockets, we rationalize the binding of DR1-restricted influenza matrix peptide IM(18–29) to DR1 subunits (Rothbard et al., 1988a) as well as peptide-induced reassembly of α- and β-chains by fluorometric HPSEC and nonreducing SDS–PAGE. Implications for the spacing of antigenic anchor residues deduced from the distance of the defined DR pockets are worked out in detail.

Experimental Procedures

Cells. The Epstein–Barr-Virus (EBV) transformed homogeneous B-cell lines WT-100 BIS (DRw 1,1) and COX (DRw 3,3) were used as a source of HLA-DR1 and HLA-DR3, respectively. Both cell lines were maintained in vitro by culture in RPMI 1640 medium supplemented with 100 μg/mL streptomycin (Gibco), 100 units/mL penicillin (Gibco), and 6% (v/v) heat-inactivated fetal calf serum (FCS) (Serva Fine Biochemicals). Cells were routinely monitored for DR expression by flow cytometry analysis. Cells were lysed at a concentration of 10^8 cells/mL by incubation for 60 min at 4 °C in the following lysis buffer: 10 mM Tris-HCl, pH 7.8, containing 0.5% (w/v) Triton X-100 (Serva), 140 mM NaCl, 1 mM $MgCl_2$ (Merck), 0.2 mM PMSF (Sigma Chemical Co.), 4 μM leupeptin, 10 μM pepstatin, and 1 μM chymostatin (Boehringer). The lysates were cleared of nuclei and debris by centrifugation at 2000*g* for 10 min. The supernatant was removed and centrifuged for an additional 60 min at 100000*g*. The homogenous supernatant was used for immunoaffinity chromatography.

Affinity Purification. HLA-DR molecules were purified as previously described by Gorga et al. (1987). Major modifications concerned the chromatographic conditions. For preparation of the immunoaffinity column the anti-DR mAb TÜ 36, a kind gift of C. Müller (Medizin. Klinik, Universität Tübingen), was covalently coupled to CNBr-activated Sepharose CL-4B (Pharmacia) at 2 mg/mL gel volume.

Cell lysates equivalent to approximately 10 g of cells were passed sequentially through the following columns: Sepharose CL-4B (10 mL) in order to remove actin and TÜ 36–Sepharose CL-4B (6 mL), recycling five times with a flow rate of 20 mL/h. The columns were equilibrated with lysis buffer and washed with 15 volumes of 10 mM Tris-HCl, pH 8.0, 140 mM NaCl, 0.05% (w/v) CHAPS (10 mL/h). HLA-DR from the TÜ 36 column was eluted with 100 mM Tris-HCl, pH 10.5, containing 0.25% (v/v) glycerol, 0.1% (w/v) CHAPS, with a flow rate of 50 mL/h. Without delay, the eluted fractions were adjusted to pH 8.0 with 6 M HCl and concentrated by ultrafiltration through a 30-kDa microsep membrane (Filtron). All purification steps were performed in the cold. Protein concentrations were determined according to the method of Bradford (1976) by using bovine serum albumin as a standard. Proteins were stored at 4 °C.

Peptide Release. Endogenous peptides and bound synthetic influenza matrix peptide(18–29), IM(18–29), were released from solubilized HLA-DR molecules according to the method of Buus et al. (1988) with slight modifications: HLA-DR preparations were adjusted to pH 4.0 with 6 M HCl and incubated for 10–30 min at room temperature. Released peptides were separated by ultrafiltration with PM 10 membranes (Amicon). Peptide-free HLA proteins (HLA-DR [REL]) were readjusted to pH 8.0 and a concentration of 1 μg/μL with 5 M NaOH and 100 mM Tris-HCl, pH 8.0, 0.05% (w/v) CHAPS. The ultrafiltrate containing the endogenous peptide fraction (EPF) was concentrated to 5 μg/mL after lyophilization and subjected to gel filtration on a Bio-Gel P-2 column (15 × 1 cm) from Bio-Rad. The column was equilibrated and eluted in 0.1% (v/v) TFA with a flow rate of 10 mL/h. The 1.2-mL fractions were lyophilized and assayed for peptides and the absence of detergent by analytical

HPLC as previously described (Kalbacher & Kropshofer, 1991).

Peptide Synthesis and Purification. IM(18–29) was synthesized by continuous-flow solid-phase peptide synthesis using a MilliGen 9050 peptide synthesizer based on Fmoc/tBu strategy (Atherton & Sheppard, 1989) and the poly(dimethylacrylamide) resin Pepsyn-K (0.1 mmol/g of resin) from MilliGen. Couplings were performed by the BOP/HOBt method (Fournier, 1988) for 30 min at a flow rate of 10 mL/min. Removal of the Fmoc group was achieved by 20% piperidine in DMF. The peptide was deprotected with TFA/thioanisole (95:5 v/v) for 3 h, precipitated with diethyl ether, and purified by preparative high-performance liquid chromatography using a 0.1% TFA/acetonitrile gradient. Integration of the analytical HPLC chromatogram (λ = 214 nm) indicated that purity was in excess of 98%. After lyophilization the peptide was analyzed by amino acid analysis and by sequencing using an Applied Biosystems 470 A sequencer. The molecular mass determined by ion spray–MS was 1324.6, compared to a calculated value of 1324.5.

AMCA Labeling of IM(18–29). Specific N-terminal fluorescence labeling was performed according to the following procedure with use of the coupling method of König and Geiger (1970): 5 μmol of 7-amino-4-methylcoumarin-3-acetic acid (Polyscience Inc., Warington) was reacted with 3.5 μmol of N^{α}-deprotected IM(18–29) peptide resin in 500 μL of DMF by adding 5 μmol of dicyclohexylcarbodiimide and 5 μmol of HOBt for 6 h in the dark at room temperature. The resin was thoroughly washed with DMF and dichloromethane and then treated with TFA/anisole/H_2O (95:3:2 v/v/v) for 12 h. The product was obtained on the addition of cold diethyl ether. Purification of the crude peptide was performed by semipreparative reversed-phase HPLC on a Nucleosil $7C_4$ column (250 × 10 mm) using a linear 0.1% TFA/acetonitrile gradient. The column effluent was simultaneously monitored at 214 nm and by fluorescence detection at λ_{ex} 350 nm and λ_{em} 450 nm. The lyophilized product showed a purity >98%, as could be demonstrated by analytical HPLC. The identity of the product was confirmed by ion spray–MS, giving the correct molecular weight of 1539.3.

Fluorescence Measurements. Fluorescence spectra were recorded at 25 °C from 300 to 390 nm on a Perkin-Elmer Model MPF-3 fluorescence spectrophotometer equipped with a Model 150 xenon lamp and a LKB Model 2210 recorder. The excitation wavelength was set at 295 nm to preferentially excite tryptophan residues. Excitation and emission resolutions were set at 5 nm. Measurements were performed in a 300-μL cuvette of 0.5-cm path length. Protein concentrations of HLA-DR1[NAT] and HLA-DR1[REL] were adjusted to 0.1 mg/mL with use of 10 mM Tris-HCl, pH 8.0/0.05% (w/v) CHAPS as a buffer. All spectra were corrected for buffer contributions. Acrylamide (Serva) and potassium iodide (Merck) were used to quench the intrinsic fluorescence of tryptophan residues. The 5 M stock solutions of acrylamide and KI, respectively, were prepared in the buffer cited above and used to adjust samples of HLA-DR to 25–200 mM acrylamide and 25–300 mM KI. To prevent oxidation of iodide, $Na_2S_2O_3$ (10^{-4} M) was added in the iodide quenching assay.

Quenching experiments were analyzed according to the classical Stern–Volmer relationship (Stern & Volmer, 1918)

$$F_0/F = K_{SV}[Q] + 1$$

where F_0 and F are the emission intensities in the absence and presence of a quencher, respectively, [Q] is the concentration of quencher, and K_{SV} is the Stern–Volmer quenching constant that can be obtained from the initial slope of the Stern–Volmer plot.

The accessibility of Trp residues to acrylamide was calculated by use of a modified Stern–Volmer equation (Lehrer, 1971) given by

$$F_0/\Delta F = 1/f_a + 1/K_Q[Q]f_a$$

where ΔF equals $F_0 - F$, f_a is the maximum fraction of the fluorophore accessible to the quencher, and K_Q is the effective quenching constant of all accessible Trp residues. Estimates for K_{SV} and f_a were calculated by using linear regression analysis done on a personal computer with SigmaPlot 4.0 (Jandel Scientific).

Circular Dichroism. CD studies were performed with a JASCO Model J-720 automatic recording spectropolarimeter interfaced and controlled by a PC data processor. HLA-DR1 preparations were measured at 0.12 mg/mL in 100 mM Tris-HCl/0.1% (w/v) CHAPS, pH 8.0 or 4.0, respectively. Spectra were recorded at 25 °C, using a quartz cell of 0.1-cm path length with a spectral bandwidth of 1 nm, a scan speed of 100 nm/min, a time constant of 4 s, and a sensitivity of 5 mdeg. The instrument was routinely calibrated by using (+)*d*-10-camphorsulfonic acid (Chen & Young, 1977). The results of five scans were averaged and corrected by subtraction of the buffer contributions. The CD data are expressed as mean residue ellipticity, $[\Theta]_R$, in deg cm^2 dmol^{-1} using the mean residue weight M_o = 139 for HLA-DR1–peptide complexes.

HPSEC Peptide Binding Assay. Aliquots of 10 μL of a diluted stock solution of HLA-DR1 or HLA-DR3, respectively (0.2 μg/mL), were coincubated with IM(18–29) with use of peptide stock solutions of 10 μg/mL in HPSEC buffer: 100 mM sodium phosphate buffer, pH 7.0, 0.05% (w/v) CHAPS. IM(18–29) was adjusted to 5 mM, assuring saturation of HLA proteins. The final assay volume was adjusted to 200 μL with HPSEC buffer. The samples were incubated for 50 h at room temperature. For HPSEC analysis, 10-μL aliquots of each sample were used. The separation was achieved on a Superose 12 HR 10/30 column (Pharmacia) equilibrated with the HPSEC buffer cited above. The column was operated at a flow rate of 0.6 mL/min and a pressure of 200 psi. For molecular weight determinations the column was calibrated by using the marker proteins thyroglobulin, rabbit IgG, BSA, ovalbumin, and myoglobin. The chromatographic system consisted of a HPLC intelligent pump Model L 6200 (Merck–Hitachi) connected to a Merck–Hitachi spectrafluorometer Model F 1050 operating at an excitation wavelength of 285 nm and an emission wavelength of 335 nm. Data were recorded by a Model D-2500 integrator (Merck–Hitachi).

Analytical Gel Electrophoresis with [AMCA]–IM(18–29). DR1[REL] and DR3[REL] (2 μM), prepared from DR1-[NAT] and DR3[NAT] as described above, were coincubated with N-terminally labeled [AMCA]–IM(18–29) (1 mM) in HPSEC buffer for 50 h at room temperature. In a parallel competition assay, identically composed samples were incubated with additional unlabeled IM(18–29) (1 mM). After the incubations the samples were loaded on a SDS–urea/13–18% polyacrylamide gradient gel prepared and run according to Laemmli (1970). Prior to fixation and silver staining, AMCA fluorescence was detected by using a transilluminator UV (365 nm) light box. A photograph was taken with the use of a 435-nm filter.

Results

Intrinsic Fluorescence of HLA-DR1 Endogenous Peptide Complexes. Acid treatment of immunoaffinity-pure MHC

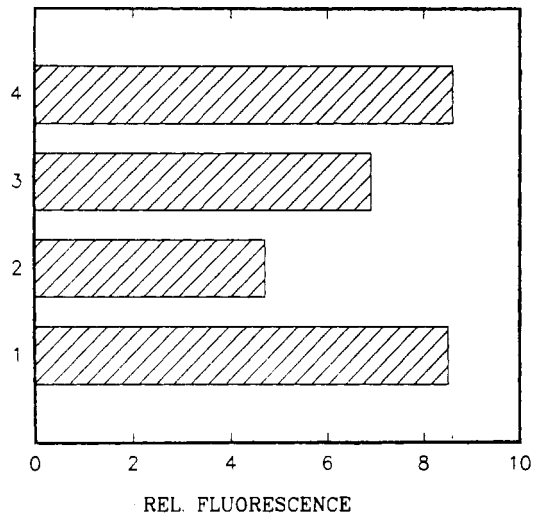

FIGURE 1: Dependence of intrinsic fluorescence of HLA-DR1 on dissociation or reassociation of endogenous peptides: (1) intact HLA-DR1–peptide complexes, pH 8.0; (2) HLA-DR1 after acid release; pH 4.0; (3) released HLA-DR1, pH 8.0; (4) HLA-DR1 after readdition of EPF, pH 8.0. Excitation was at 295 nm; emission was at 335 nm. HLA-DR1 and EPF were in 10 mM Tris-HCl, pH 8.0 or 4.0, containing 0.05% (w/v) CHAPS at 25 °C.

molecules releases tightly bound endogenous peptides, as previously shown by Buus et al. (1988). The same procedure applied to HLA-DR1 is accompanied by a sharp decrease in intrinsic Trp fluorescence (Figure 1). Readjusting the release sample to pH 8.0 increases the fluorescence signal, but the final intensity is about 18% smaller than the initial one. Separation of the EPF, the molecular weight limit being ≤10 kDa, readdition of the EPF in a 20-fold molar excess to HLA-DR1[REL], and coincubation for 48 h completely restores the initial fluorescence, reaching 108% of the initial intensity.

Acrylamide Quenching. With use of an excitation wavelength of 295 nm HLA-DR1[NAT] shows a very strong fluorescence signal due to its nine tryptophan residues (Figure 2a). The contribution of the 13 tyrosine residues in the wavelength range 330–360 nm is negligible, as could be evidenced by comparing the emission spectra recorded with λ_{ex} 280 nm, λ_{ex} 285 nm, and λ_{ex} 295 nm, respectively (not shown). In each case a broad maximum appears around 338 nm. Upon quenching with 0.2 M acrylamide the maximum is blue-shifted to 336 nm, its intensity decreasing about 30%. The difference spectrum shows a shallow maximum at 350 nm, being typical for Trp residues that are fully exposed to aqueous solvents. The emission spectrum of HLA-DR1[REL]—prepared by a 10-min release, as described above—is dominated by a narrow maximum at 340 nm that is shifted to 338 nm and quenched about 40% by acrylamide (Figure 2b). The difference spectrum, peaking at 345 nm, further indicates that HLA-DR1-[REL] bears additional Trp residues, with their accessibility to acrylamide obviously being different from the comparable Trp fraction of HLA-DR1[NAT]. The nonlinearity of the Stern–Volmer plots, characterizing the response after successive addition of acrylamide, clearly demonstrates that the Trp residues of both DR1 species can be classified in at least two populations (Figure 3a). Both plots show downward curvature, the initial slopes being nearly identical (Table I): $K_{SV;DR1[NAT]}$ = 23.6 M^{-1} and $K_{SV;DR1[REL]}$ = 17.1 M^{-1}. With more than 50 mM acrylamide added, the plots differ markedly in their slopes: DR1[NAT] is quenched with 3.3 M^{-1}, whereas K_{SV} of DR1[REL] is more than the double of it (7.2 M^{-1}). The quantitation of these data in the modified Stern–Volmer plots yields the following results (Table I): 59.3%, corresponding to five Trp residues of DR1[NAT], are accessible to the surface quencher acrylamide, whereas release of peptides exposes an additional 19.8% of the Trp fluorophores. That means that two Trp residues become accessible to acrylamide upon acid release of self peptides.

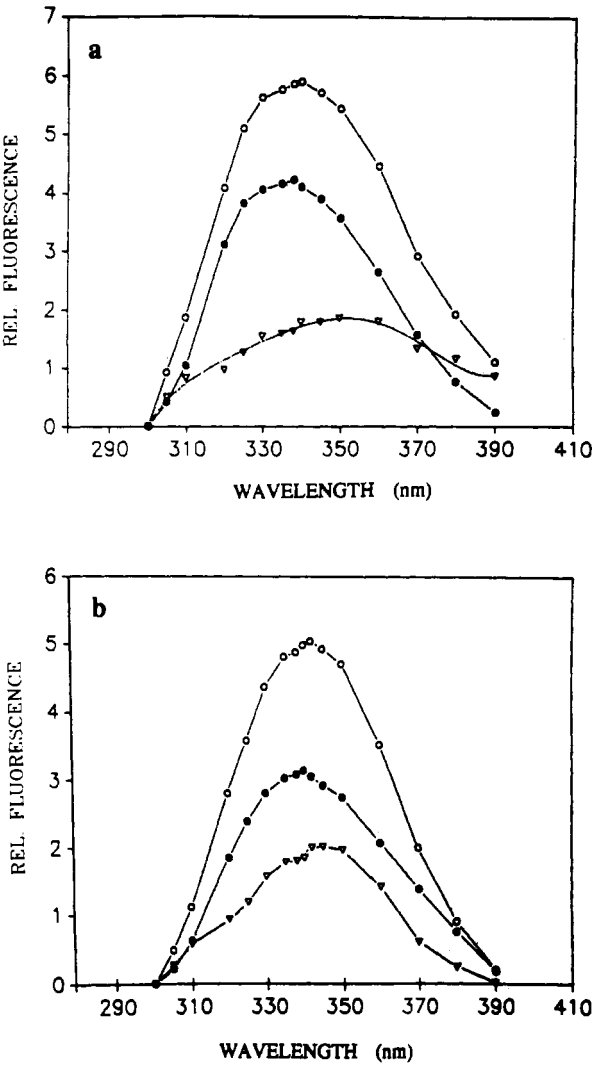

FIGURE 2: Fluorescence emission spectra of HLA-DR1[NAT] (a) and HLA-DR1[REL] (b) in the absence (○) and presence (●) of 0.2 M acrylamide. The third curve denotes the difference spectrum (▽). Excitation was 295 nm. Measurements were in 10 mM Tris-HCl, pH 8.0, containing 0.05% (w/v) CHAPS at 25 °C.

Table I: Acrylamide and Iodide Quenching of HLA-DR1: Quenching Constant K_{SV} and Trp Fraction Accessible to Quencher (f_a)

	K_{SV} (1/M)						
	acrylamide		iodide	f_a (%)		n_{Trp}	
	t_o	$t_{\gg o}$	t_o[a]	acrylamide	iodide	acrylamide	iodide
HLA-DR1-[NAT]	23.6	3.3	1.3	59.3	40.0	5	4
HLA-DR1-[REL]	17.1	7.2	1.2	79.1	45.7	7	4

[a] t_o denotes the initial and $t_{\gg o}$ denotes the noninitial slope of the biphasic Stern–Volmer plot; n_{Trp} denotes the number of Trp residues accessible to the quencher.

Iodide Quenching. The influence of the charged quencher iodide on the fluorescence intensity of DR1 is shown in Figure 4a. The Stern–Volmer plots of DR1 before and after peptide release are nearly identical: both plots are characterized by a slight downward curvature, the initial slope being about 1.1 M^{-1} (Table I). The modified Stern–Volmer plots confirm these

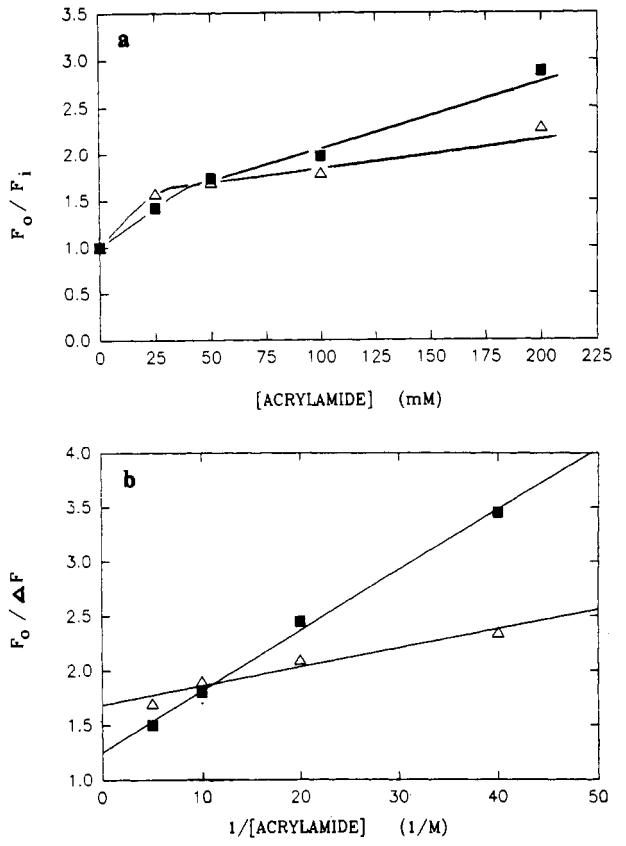

FIGURE 3: Stern–Volmer plots (a) and corresponding modified Stern–Volmer plots (b) for quenching by acrylamide of intrinsic Trp fluoresence of HLA-DR1[NAT] (△) and HLA-DR1[REL] (■). Excitation was at 295 nm; emission was monitored at λ_{max} of emission. Measurements were in 10 mM Tris-HCl, pH 8.0/0.05% (w/v) CHAPS at 25 °C.

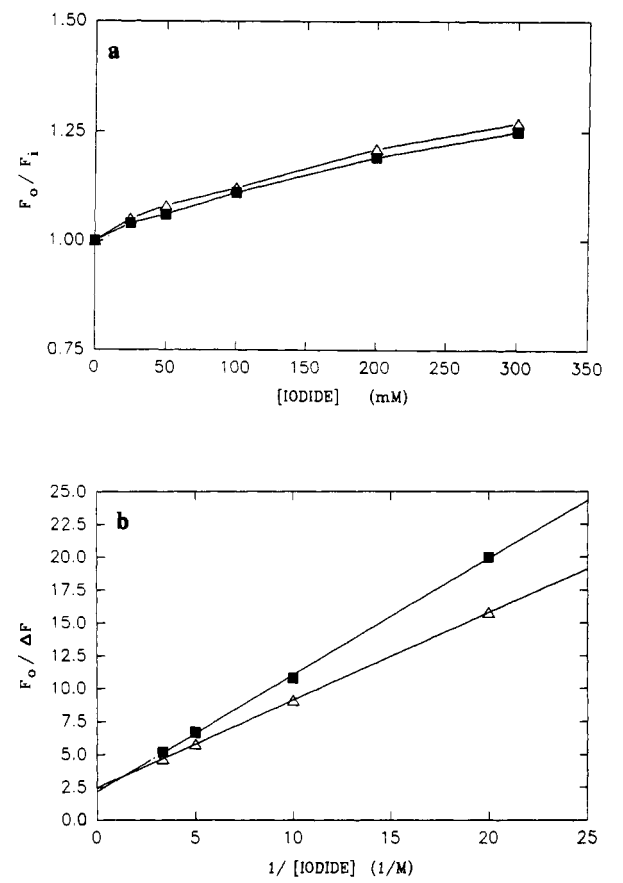

FIGURE 4: Stern–Volmer plots (a) and corresponding modified Stern–Volmer plots (b) for quenching by iodide of Trp fluorescence of HLA-DR1[NAT] (△) and HLA-DR1[REL] (■). Excitation was at 295 nm; emission was monitored at λ_{max} of emission. Measurements were in 10 mM Tris-HCl, pH 8.0/0.05% (w/v) CHAPS, 25 °C.

results. The regression analysis yields 40.0% accessibility for the total Trp population for DR1[NAT] and 45.7% for DR1[REL] (Table I). Therefore, peptide release leaves the number of four Trp residues accessible for iodide more or less unchanged.

CD Spectroscopic Analysis of DR1[NAT] and DR1[REL]. Solubilization of isolated HLA-DR1 in Tris buffer, containing CHAPS at concentrations below the critical micellar concentration, made CD measurements possible without prior proteolytic elimination of the membrane anchor, as previously reported by Gorga et al. (1989). However, the detergent precluded collection of data at wavelengths less than 200 nm. The far-UV CD spectra (200–260 nm) of HLA-DR1 before (DR1[NAT]) and after peptide release (DR1[REL]) at 5 °C are shown in Figure 5. The spectrum of DR1[NAT] has a pronounced double minimum at $\lambda_1 = 210$ and $\lambda_2 = 220$ nm, indicating a considerable portion of α-helical conformation. Both minima are broad, their distance being rather small ($\Delta\lambda = 10$ nm). These are features expected for proteins containing additional ordered structures, especially β-pleated sheets and β-turns. The spectrum of DR1[REL] is dominated by a single broad minimum at 214 nm touching the curve of DR1[NAT] at this wavelength, whereas the ellipticities of the previous minima at λ_1 and λ_2 decreased by 800–900 deg cm^2 dmol^{-1}, respectively. The comparison of these data with those recorded at 25 °C (Table II) shows far-reaching identity at 222 nm. The conformational analysis yields 22.9 ± 1.0% helicity for DR1[NAT] and 20.7 ± 0.4% helical content for DR1[REL] (Table II). Therefore, the helicity decreased by ~2.2% upon release of peptides. The deviations in the sheet content are somewhat greater: the spectra recorded at 5 °C show a 15% higher portion of pleated sheets compared to those at 25 °C. But the differences upon acid peptide release are ≤1%. The

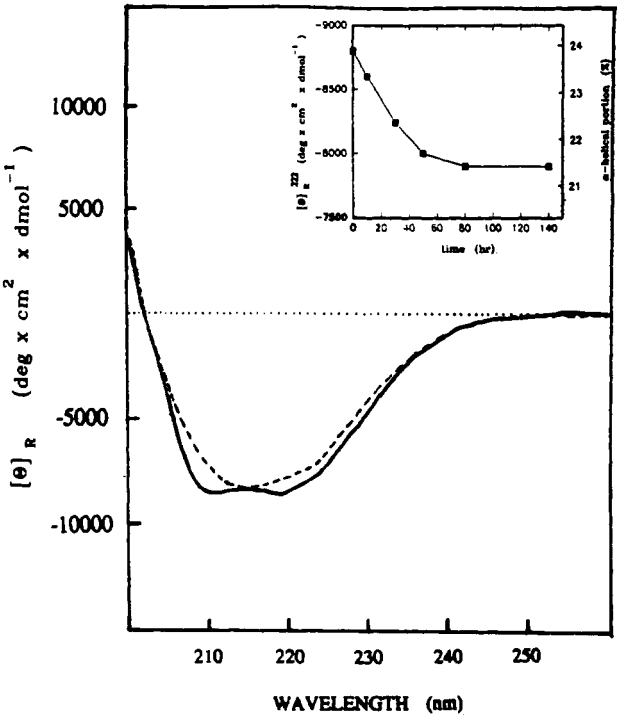

FIGURE 5: Circular dichroism spectra of HLA-DR1[NAT] (—) and HLA-DR1[REL] (– –), 0.12 mg/ML, respectively, after a 140-h release, pH 4.0, 25 °C. The spectra were taken in 10 mM Tris-HCl, pH 8.0/0.1% (w/v) CHAPS at 5 °C. The kinetics of the release at 25 °C is shown in the inset.

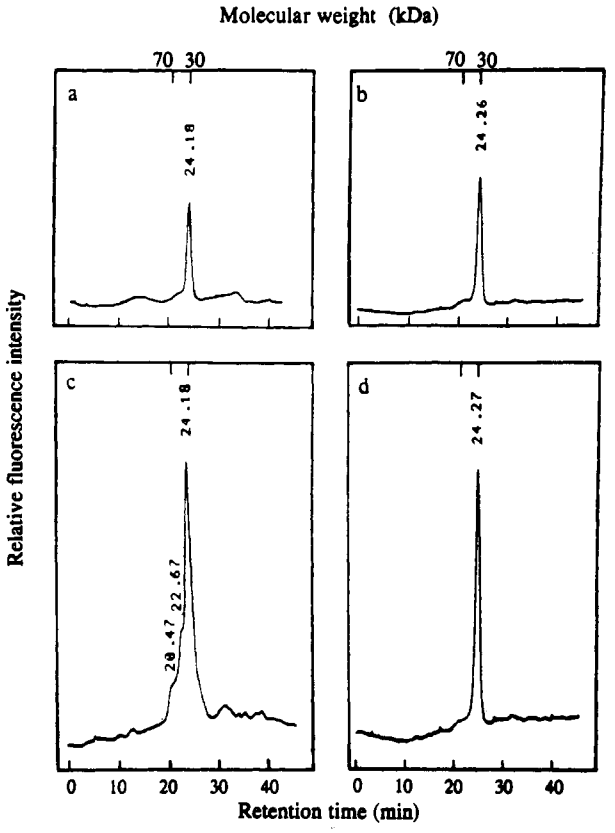

FIGURE 6: HPSEC fluorescence chromatograms of dissociated HLA-DR1[REL] (a) and HLA-DR3[REL] (b) after a 50-h coincubation with IM(18–29) (c and d) on a Superose 12 HR 10/30 column. Sample size: 20 μL. Flow rate: 0.6 mL/min. HLA-DR proteins (3 μM) and IM(18–29) (10 mM) were incubated and chromatographed in 50 mM phosphate buffer, pH 7.0/0.1% (w/v) CHAPS at 25 °C. The ordinate is fluorescence at 335 nm in arbitrary units.

Table II: CD Spectroscopic Data and Hypothetical Conformational Parameters of Human Class II Proteins According to Brown et al. (1988)

	temp (°C)	$[\theta]_{222} \times 10^{-3}$ [a]	$[\theta]_{202} \times 10^{-3}$ [a]	f_α [b]	f_β [b]
HLA-DR1-[NAT]	5	−8.1	0.8	0.219	0.535
	25	−8.8	−1.1	0.239	0.386
HLA-DR1-[REL]	5	−7.5	0.8	0.202	0.535
	25	−7.9	−1.2	0.213	0.378
hypothetical model				0.211[c]	0.332[c]

[a] Mean residue ellipticity (in deg cm^2 dmol^{-1}) of HLA-DR1 at 202 and 222 nm. [b] The contents of helix (f_α) and β-pleated sheet (f_β) were calculated according to Greenfield and Fasman (1969), from the following equations: $f_\alpha = ([\theta]_{222} - [\theta]_\alpha)/([\theta]_h - [\theta]_\alpha)$ with $[\theta]_\alpha = -36\,000$ deg cm^2 dmol^{-1} and $[\theta]_\alpha = -260$ deg cm^2 dmol^{-1}; $f_\beta = ([\theta]_{202} - [\theta]_\beta)/([\theta]_f - [\theta]_\beta)$ with $[\theta]_f = 6700$ deg cm^2 dmol^{-1} and $[\theta]_\beta = -6000$ deg cm^2 dmol^{-1}. [c] The theoretical values for f_α and f_β were calculated with use of the reported α-helix and β-sheet contents of HLA-A2 (Bjorkman et al., 1987).

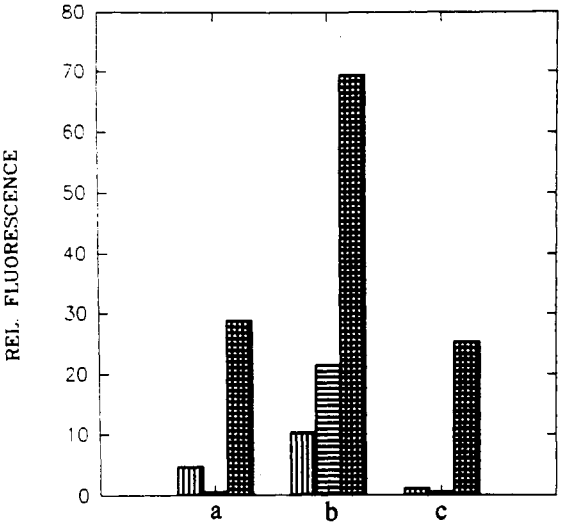

FIGURE 7: HPSEC analysis of association and dissociation of HLA-DR1–IM(18–29) complexes. HLA-DR1[NAT], 5 μM (a), and nonfluorescent IM(18–29), 1 mM, after coincubation for 50 h, form bi- and trimolecular complexes (b) that dissociate upon HCl treatment (pH 4.0, 10 min, 25 °C) (c). Incubation and chromatography were performed in 50 mM phosphate buffer, pH 7.0/0.1% (w/v) CHAPS at 25 °C. Excitation was at 295 nm; emission was monitored at 335 nm. Key: vertical lines, 65-kDa dimer peak (floppy conformer); horizontal lines, 55-kDa dimer peak (compact conformer); vertical and horizontal lines, 30-kDa monomer peak.

CD spectroscopic kinetics of the release at 25 °C (insert of Figure 4) shows that the 2.2% decrease of helicity proceeds very slowly, reaching a constant value after 80 h.

HPSEC Peptide-Binding Assay. Release of endogenous peptides by acid treatment is supposed to destablize the noncovalently associated α- and β-subunits of heterodimeric MHC class II proteins. The chromatographic proof of the dissociation of the dimer is illustrated in parts a and b of Figure 6: the chromatograms of DR1[REL] and DR3[REL] show single peaks, the corresponding apparent molecular mass being 30 kDa. The equivalent of the heterodimer disappears nearly quantitatively. Coincubation of both the two released HLA-DR isoforms with saturating concentrations of the DR1-restricted T-cell epitope IM(18–29) and analysis by the previously introduced fluorometric assay (Kalbacher & Kropshofer, 1991) result in the chromatograms shown in parts c and d of Figure 6. Since the release of peptides correlates with a decrease of intrinsic Trp fluorescence we expected an increase of fluorescence intensity after binding IM(18–29). The fluorescence intensity of the monomer peak of DR1 increases considerably; in addition, two shoulders appear, their apparent molecular mass being 55 and 65 kDa, respectively. The 65-kDa species elutes with the retention time of a common dimeric DR molecule (cf. Figure 7). The 55-kDa species mirrors the floppy conformer of DR, originally described by Dornmair et al. (1989). In contrast, with DR3 the reconstitution of dimeric MHC species by high-affinity binding of IM(18–29) is not

Table III: HPSEC Peptide Binding Assay: Binding of IM(18–29) to HLA-DR1[REL] and HLA-DR3[REL], Respectively

	rel fluorescence intensities (arbitrary units)			
	DR1[REL]	DR1[REL] + IM(18–29)	DR3[REL]	DR3[REL] + IM(18–29)
monomers (F_{1i})	540 (100%; i = 1)	1490 (75%; i = 2)	770 (100%; i = 3)	1390 (100%; i = 4)
dimers (F_{2i})		510 (25%; i = 2)		
$\Delta F_1 = F_{12} + F_{22} - F_{11}$		1460		
$\Delta F_2 = F_{14} - F_{13}$				620
$\Delta F_3 = F_{12} - F_{11}$		950		
$\Delta\Delta F_1 = \Delta F_1/\Delta F_2$		2.35		
$\Delta\Delta F_2 = \Delta F_3/\Delta F_2$		1.53		

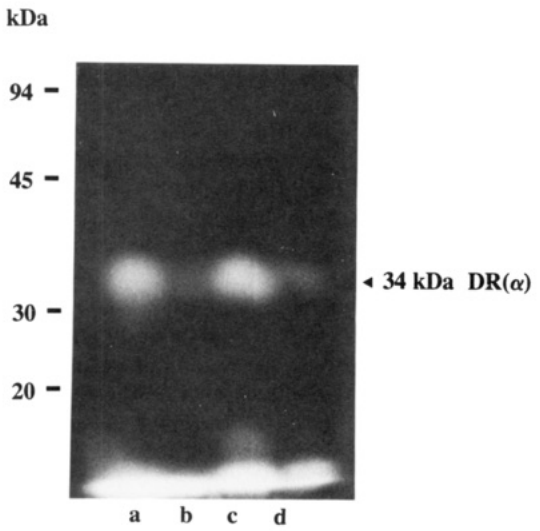

FIGURE 8: SDS–PAGE with fluorescence detection showing specific binding of IM(18–29), N-terminally labeled with AMCA, to the α-chain of DR1 and DR3, respectively. DR1[REL] and DR3[REL] (2 μM) and [AMCA]–IM(18–29) (1 mM) were coincubated for 50 h at room temperature and loaded on a nonreducing SDS–urea gradient gel of 13–18% acrylamide. Lane a, DR1 + [AMCA]–IM-(18–29); lane b, DR1 + [AMCA]–IM(18–29), competition with IM(18–29); lane c, DR3 + [AMCA]–IM(18–29); lane (d) DR3 + [AMCA]–IM(18–29), competition with IM(18–29).

possible. Nevertheless, binding to monomeric DR3 is evidence by a significantly growing monomer peak (Figure 6d). Table III summarizes the HPSEC data by comparing the integrated fluorescence peak areas of DR1 and DR3 before and after binding of IM(18–29). A closer view of the increase of the total fluorescence (ΔF_1 and ΔF_2) and the monomer signals (ΔF_2 and ΔF_3) of DR1 and DR3, respectively, reveals characteristic and reproducible ratios: $\Delta\Delta F_1 = \Delta F_1/\Delta F_2 = 2.35$, whereas $\Delta\Delta F_2 = \Delta F_3/\Delta F_2 = 1.53$.

Release of DR1-Bound IM(18–29). DR1[NAT] also dissociates into its subunits upon dilution (≤0.1 mg/mL) and prolonged storage at 4 °C. This is accompanied by partial release of bound peptides (not shown). A typical preparation of this kind was used in the HPSEC assay illustrated in Figure 7. The initial sample consisted of 20% heterodimeric and 80% monomeric HLA-DR1, represented by a 65-kDa and a 30-kDa peak, respectively (Figure 7a). After binding of IM(18–29), we observe the same differential increase of fluorescence as described in Figure 6c: a very strong growing 30-kDa monomer peak, the induction of the 55-kDa compact conformer, and the doubling of the intensity of the 65-kDa dimer peak (Figure 7b). The greater portion of dimeric species (30%) compared to the HPSEC assay with totally dissociated DR1[REL] (25%; Table III) obviously originates from preexisting initial dimeric molecules. Acid treatment of DR1–IM(18–29) complexes results in total disappearance of the 55-kDa peak and 85% and 55% reduction of the 65- and 30-kDa peaks, respectively (Figure 7c).

SDS–PAGE Assay with [AMCA]–IM(18–29). The detection of AMCA fluorescence in the gel in Figure 8 shows a single intensive signal in lanes a and c, respectively, corresponding to 34 kDa, as could be verified by molecular weight markers after silver staining (not shown). The area and the intensity of the signal indicate that [AMCA]–IM(18–29) binds equally well to the α-chains of DR1 and DR3, respectively, using the peptide in a 500-fold molar excess. This result confirms the cellular assay of Ceppellini et al. (1989) showing significant binding of the IM(17–29) ^{125}I-Tyr to the DR 3,3 cell line STEINLIN. In addition, our assay demonstrates specific binding of [AMCA]–IM(18–29) since unlabeled IM-(18–29), in the case of DR1 and DR3, successfully suppresses binding of the labeled peptide (lanes b and d).

Discussion

Since a high-resolution crystallographic analysis of a class II MHC molecule is not available yet, our aim was to search for alternative methods to reveal the structural features of the single peptide-binding groove that restrict high-affinity binding to certain peptide-specific sequence motifs. In this context, we developed a highly sensitive binding assay, based on the intrinsic Trp fluorescence of human class II MHC proteins (Kalbacher & Kropshofer, 1991). Our present study focuses on the fluorescent response of DR1 molecules upon release and binding of endogenous or foreign peptides.

Figure 1 shows that the acid release of endogenous peptides from HLA-DR1 proceeds by a significant reduction of Trp fluorescence, the maximum red shifting from 338 to 340 nm (Figure 2). We conclude that a certain portion of the nine-residue Trp population of DR1 becomes more exposed to the polar exterior upon dissociation of self peptides. This could be due to long-range tertiary structural changes concerning Trp residues far away from the peptide-binding site or to short-range conformational rearrangements in the groove or to the peptide itself contacting Trp residues in the bound state. The fact that the fluorescence change of 18% increases to a nearly 4-fold value releasing preformed DR1–IM(18–29) complexes (Figure 7), strongly favors two notions: (i) the fluorescence intensity is directly dependent on the specific side chains of the peptide interacting with the relevant fluorophores; and (ii) the fluorescence signal originates from the HLA molecule since IM(18–29) is a nonfluorescent peptide. The increase of the fluorescence to 108% of the original intensity of DR1[NAT] after saturating readdition of an EPF supports the explanation above and confirms previous reports, whereafter 85–99% of class II MHC proteins are filled with self peptides (Chen & Parham, 1989; Ceppellini et al., 1989). Quenching with acrylamide and iodide enables us to quantitate and characterize those Trp residues that are buried after peptide binding. The difference spectra of Figure 2 demonstrate that the quenching efficiency of 0.2 M acrylamide grows from 30% before to 40% after peptide release. Acrylamide is a surface quencher; therefore, additional Trp residues must have been exposed to the solvent as a consequence of peptide liberation. However, the new solvent-accessible Trp population seems to be partly buried in a hydrophobic crevice, since the maximum of the difference spectrum is blue-shifted from 350 nm—typical for fully exposed Trp residues—to 345 nm. The remaining quenching data obtained with acrylamide and iodide support this view. Taking the rule, the higher the Stern–Volmer quenching constant K_{SV} the greater the Trp exposure, for granted, DR1[NAT] and DR1[REL] have four Trp residues in common, as concerns their location and their chemical neighborhood. They are quenched with $K_{SV} = 1.2\ M^{-1}$ by the charged quencher iodide and are likely to contribute to the strong initial quenching effect of acrylamide, with $K_{SV} = 17.1–23.6\ M^{-1}$ (Table I). Five other tryptophans are not accessible to iodide at all, but two of them seem to get accessible to acrylamide upon peptide release, with $K_{SV} = 7.2\ M^{-1}$, indicating that they are weakly exposed to the solvent. Obviously, iodide is not able to quench the fluorescence of the two additionally exposed Trp residues. With iodide having a large ionic volume, hydrophilic nature, and a negative charge, its penetration to narrow and hydrophobic crevices or pockets of the HLA molecule is expected to be rather low. Thus, the most reasonable explanation for our quenching results is that

Table IV: Homologous Specificity Pockets in HLA-A2, HLA-Aw68, HLA-DR1, and HLA-DR3

	HLA-A2			HLA-Aw68			HLA-DR1			HLA-DR3		
	p[a]	d	c	p	d	c	p	d	c	p	d	c
	A-24			A-24			F-26			F-26		
	G-26			G-26			G-28			G-28		
I	V-34	α_1	●	V-34	α_1	●	V-34	α_1	●	V-34	α_1	●
	M-45			M-45			W-43			W-43		
	V-67			V-67			A-59			A-59		
	H-74	α_1		D-74	α_1		N-69	α_1		N-69	α_1	
	V-95	α_2		I-95	α_2		W-9	β_1		E-9	β_1	
II	R-97	α_2	○	M-97	α_2	○	L-11	β_1	●	S-11	β_1	○
	Y-116	α_2		D-116	α_2		C-30	β_1		H-30	β_1	
	Y-118	α_2		Y-118	α_2		Y-32	β_1		H-32	β_1	
	I-124			I-124			V-38			A-38		
	W-133			W-133			Y-47			Y-47		
III	W-147	α_2	●	W-147	α_2	●	W-61	β_1	●	W-61	β_1	●
	Q-153			Q-153			L-67			L-67		

[a] p, position, taken from Brown et al. (1988); d, domain; c, chemical character shown as hydrophobic (●) or polar (○).

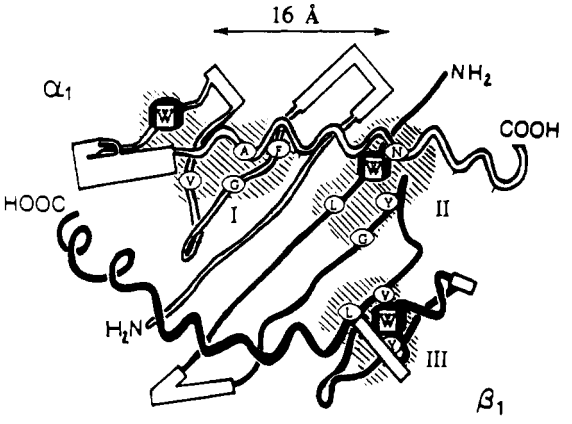

FIGURE 9: Location of the three proposed Trp pockets (I–III) in a schematic drawing of the predicted α-carbon structure of the heterodimeric HLA-DR1 molecule. The structure is based on the hypothetical model of Brown et al. (1988).

at least two of the nine Trp residues of DR1 are located in two hydrophobic pockets of the peptide-binding groove, with self peptides shielding them from access of acrylamide in DR1[NAT]. Garrett et al. (1989) provided crystallographic proof for the existence of "specifity pockets" in the binding cleft of class I molecules HLA-Aw68 and HLA-A2. The constituting residues of some of those pockets are polymorphic and seem to be responsible for allelic specifity in peptide affinity. Table IV compiles the amino acids and the chemical character of the three most prominent pockets of HLA-Aw68 and HLA-A2: the Met-45 pocket (I), the Asp-(His)-74 pocket of Aw68 (A2) (II), and the Trp-133 pocket (III). The list also contains the corresponding positions of the class II isotypes DR1 and DR3 according to the class II model of Brown et al. (1988). Provided the cited residues are similarly located, DR1 is characterized by three hydrophobic pockets, each of them possessing a central Trp residue. DR3 differs from DR1 only in pocket II: Glu-9(β_1) replaces Trp-9(β_1), with the other residues of the pocket also being polar or charged. Hence, DR3 compares to A2 and Aw68 owing to two hydrophobic and one polar pocket, whereas all three postulated pockets of DR1 are hydrophobic. Figure 9 illustrates the hypothetical location of the three DR1 pockets. Pocket I, with a central Trp-43(α_1), is formed by contributions of three β-strands and Ala-59(α_1) of the N-terminal half of the α_1-helix. Pockets II and III with the central Trp-9(β_1) and Trp-61(β_1), respectively, are positioned approximately 16 Å distant from

Table V: Peptide Amino Acid Sequences in the Single-Letter Code and Alignment According to the Two-Residue-Contact Model of the DR1-Restricted Peptides IM(18–29), HA(306–318), CS(381–393), TUB(3–14), and the Nonbinding Peptide TT(763–775) from Tetanus Toxoid[a]

peptide	sequence	binding capacity
Influenza matrix protein IM(18-29)	GP L KAEIAQR L E	+
Hemagglutinin HA(306-318)	PK Y VKQNTLK L AT	+
	PKY V KQNTLKL A T	+
Circumsporozoite protein CS(381-393)	KKI A KMEKASS V F	+
M. tuberculosis protein TUB(3-14)	R V KRGLTVA V AG	+
Tetanus toxin TT(763-775)	GP D KEQIADE I N	−

[a] The residues representing the postulated DR1 restriction motif are boxed. Identical residues between IM(18–20) and TT(763–775) are underlined.

pocket I. Whereas pocket III is built up very similarly to pocket I, pocket II is composed of portions of both subunits: N-69 from the α_1-helix of the α-chain, with the remaining three residues belonging to two β-strands of the β-chain.

There are several lines of evidence that the proposed class II pocket residues (Table IV) do interact with side chains of antigenic peptides: Berzofsky et al. (1990) have shown with site-directed mouse I-A^k mutants that substitution at position 9(β_1) abrogates binding of I-A^k-restricted myoglobin peptide(122–130). Peccoud et al. (1990) have recently exchanged residues 56–79 of the α-chain of I-A^k step by step for Ala with a set of 30 L-cell transfectants. They reported that substitutions at position 59(α_1) or 69(α_1)—residues of the hypothetical pockets I and II, respectively, not being accessible to anti-I-A^k(α) antibodies—lowered presentation of HEL(46–61) to various T-hybridomas drastically. Jardetzky et al. (1990) have found in a peptide-based Ala-exchange assay that Tyr-308 of DR1-restricted peptide HA(306–318) and at least one additional hydrophobic residue are contact sites sufficient and essential for high-affinity binding to HLA-DR1. This result fits very well with our proposed pocket model of DR1, whereafter two appropriately spaced nonpolar residues of the peptide contact two of the three hydrophobic pockets. In the case of IM(18–29), taking into account that the peptide adopts an α-helical conformation in the DR1-bound state (Rothbard et al., 1988), Leu-20 and Leu-28 are likely to be anchor residues that fit into pocket I and pocket II or III (Table V). The distance of 16 Å between two pockets is spanned by $2^1/_2$ helical turns, making 13 Å; the remaining 3 Å can be covered by both of the Leu side chains. Corresponding potential contact residues of HA(306–318) according to our pocket hypothesis are Tyr-308 and Leu-316, lying $\Delta n = 8$ residues apart, as well. Ala-317 together with Val-309, leaving $\Delta n = 8$ constant, might substitute for Tyr-309/Leu-316, since all single substitutions made for Leu-316 showed full activity in T-cell assays (Rothbard et al., 1989). Binding assays of Busch and Rothbard (1990) with purified DR4 and HA(306–318) have shown a minimum length requirement of about 10 residues, just comprising the minimum length of $n = 9$ we have to claim for our two-residue-contact model. T-cell epitopes of circumsporozoite protein, CS(381–393) (Sinigaglia et al., 1988), and *M. tuberculosis*, TUB(3–14) (Hickling et al., 1990), obey the same sequence motif (Table V). On the other hand, our assumption rationalizes why tetanus toxin peptide(763–775), although sharing five residues with IM(18–29), does not bind to the antigen-binding site of DR1 (Jardetzky et al., 1990). The alignment reveals that the equivalent anchor

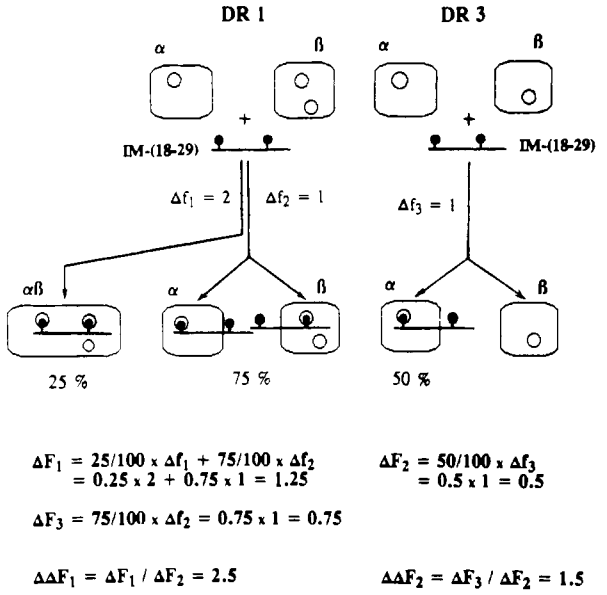

FIGURE 10: Rationale for the HPSEC binding data with IM(18–29), DR1, and DR3. DR subunits are symbolized by rectangles; small open circles indicate the postulated pockets (cf. Figure 9). Small filled circles of IM(18–29) symbolize anchor residues according to the two-residue-contact model. Δf_i denotes the number of Trp residues per binding unit that interact with the peptide anchors. ΔF_i and $\Delta\Delta F_i$ are defined as in Table III.

positions should be Asp-766 and Ile-774 (Table V). Ile-774 obeys our rule, but the charged and polar Asp-766 is bound to be excluded from each of our three pockets, abolishing the formation of stable DR1–TT(763–775) complexes. High-affinity binding epitopes such as IM(18–29) are even able to bind to disassembled DR1 and DR3 proteins, as could be demonstrated in our HPSEC assay (Figure 6) as well as by nonreducing SDS–PAGE with fluorescently labeled IM(18–29) (Figure 8). Acid release of endogenous peptides destabilizes DR1 and DR3 heterodimers, resulting in uniform 30-kDa signals of monomeric α- and β-chains (Figure 6a,b). The characteristic growing of the monomer peak of DR1 (ΔF_3) and DR3 (ΔF_2), respectively, upon binding IM(18–29) is explained in the diagram of Figure 10, assuming that (i) DR1 and DR3 bind IM(18–29) equally well under saturating concentrations of peptide, as could be verified by SDS–PAGE (Figure 8a,c) and (ii) the quantum yields of all the relevant Trp residues in the binding sites of DR1 and DR3 are comparable, since they are all located in uniform hydrophobic pockets (Table IV), the ratio $\Delta\Delta F_2 = \Delta F_3/\Delta F_2 = 1.53$ (Table III) must be ascribed to pocket II, the only pocket in which DR1 and DR3 differ (Table IV). Binding of IM(18–29) to the α-chain of DR1 as well as DR3 via pocket I, respectively, and, independently, to the β-chain via pocket II gives a theoretical value of $\Delta\Delta F_2 = 1.5$ (Figure 10). Judging from the monomer signals alone, we cannot exclude formation of DR3(β)–IM(18–29) complexes because pocket II of DR3 bears no Trp residues, thereby providing no fluorescence signal. Most probable, binding to both of the disassembled subunits leads to partial reassociation of the $\alpha\beta$ heterodimer (25%), as observed only with DR1 (Figure 6c). In this case, IM(18–29) may function as a bridging peptide. The two neogenerated dimer species with 55 and 65 kDa apparent molecular masses are likely to be the HPSEC equivalents of the reported compact and floppy conformers in the SDS–PAGE analyses of Dornmair et al. (1989). Since dimerization obviously did not occur with DR3 (Figure 6d), IM(18–29) solely binding to the α-chain of DR3[REL] is more realistic. The proviso of our quenching experiments, that two Trp pockets are occupied upon peptide binding ($\Delta f_1 = 2$) also explains the ratio $\Delta\Delta F_1 = \Delta F_1/\Delta F_2$ that compares the intensities of the monomer- and dimer-fluorescence signals after binding IM(18–29). With the $\alpha\beta$ dimers of DR1 covering 25% of the total fluorescence, the calculated value of $\Delta\Delta F_1$ equals 2.5 (Figure 10), pretty close to the experimentally deduced value of 2.35 (Table III). Our SDS–PAGE assay using [AMCA]–IM(18–29) verifies high-affinity and specific binding of IM(18–29) to the α-chain of DR1 and DR3, respectively, with unlabeled IM(18–29) inhibiting binding very effectively (Figure 8). In contrast to our HPSEC results, binding to the β-chain could not be demonstrated either for DR1 or for DR3. The reason could be that pocket II, which is responsible for binding to the β-chain according to our two-residue-contact model, is built up by residues of both subunits. Therefore, after disassembly of the subunits pocket II is not in its native state any longer, whereupon formation of labile DR(β)–IM(18–29) complexes occurs. Consequently, these complexes, if ever formed, are prone to dissociate under gel running conditions. Another explanation might be that the N-terminal AMCA fluorophore of IM(18–29) sterically hindered the interaction of the β-chain pocket with the corresponding anchor residue. Consequently, no reassociation of dimers could occur, and that is what we get in our gel assay.

Dornmair et al. (1989), who did the first fluorescence gel-scanning experiments showing association of cyt *c* peptide(88–104) to I-A^d subunits without prior cross-linking, noticed that binding is only possible provided that binding sites do not undergo significant changes during diassembly. We can confirm this notion by our CD spectroscopic analysis (Table II): the α-helix and β-sheet contents of DR1[NAT] are both reduced by only 1–2% under prolonged peptide release conditions, with the reduction of helicity proceeding with extremely slow kinetics (Figure 4). Hence, association and dissociation of peptides probably involves the formation of conformational reaction intermediates, as previously proposed by Sadegh-Nasseri and McConnell (1989). Besides that, dissociation of helical endogenous peptides that are folded randomly in aqueous solution due to their short length may partly contribute to the decrease of helicity. In addition, the CD data provide further evidence for the reliability of the hypothetical class II model: thereafter the portions of α-helix and β-sheet equal 21% and 33%, respectively. These values fit very well with 21–24% and 38%, measured at 25 °C. Our data supplement similar CD results of Gorga et al. (1989), who analyzed papain-solubilized DR1 proteins, with the experiment suffering from the fact that the papain cleavage sites have not been defined until now.

Taking the HPSEC and the CD analyses together, we conclude that dissociation of endogenous peptides after acid treatment is followed by disassembly of the α- and β-chains, albeit leaving the overall secondary structure of both subunits unaltered. After readjusting neutral pH, binding of T-cell epitopes to disassembled α- or β-chains is possible. For peptide loading of class II MHC proteins in vivo this implies that after posttranslational modification of de novo synthesized α- and β-chains a certain ER-resident endogenous peptide population might get into contact with both chains before Ii binds to the so-formed $\alpha\beta$ heterodimer–peptide complexes. Viguier et al. (1990) have given evidence for the existence of tetrameric complexes involving α, β, and Ii chains and antigenic peptides in vivo. Inhibition studies of Nuchtern et al. (1990) with brefeldin A and chloroquin indicated that both class I and class II molecules can complex with antigenic peptides in a pre-Golgi compartment. A unified mechanism for the presentation of

endogenous peptides starting from the ER also could account for various reports on allogeneic presentation of MHC-derived alloantigens (Saskia de Koster et al., 1989; Olson et al., 1989).

As a summary, our investigations enable us to expand the functional analogy and the proposed structural homology between HLA class I and II proteins to the occurrence of specifity pockets in the antigen-binding groove. As evidenced for HLA-DR1, the number, allele-specific chemical character, and location of the pockets determine the sequence motif that makes selection of certain peptides out of a vast cellular pool possible. The introduced two-residue-contact model associates two HLA pockets with two complementary residues of antigenic peptides. The spacing of the anchor residues depends on the conformation the peptide adopts in the binding groove. The conformation of the peptide seems to be primarily determined by the residues between the anchor positions. In the case of HLA-DR1, the distance between the anchor side chains is approximately 16 Å. Since prominent high-affinity binding DR1-restricted peptides as IM(18–29), HA(306–318), and CS(381–393) are supposed to adopt helical conformation in the bound state, seven residues are interspaced between the contact sites, limiting the minimal peptide length to 9–10 residues. The length of N- or C-terminal presequences seems to be variable, in general. Differences in binding affinity and restriction might be ascribed to the differential grade of fitting between anchor residues and contact sites of the pockets and, in addition, to the existence of a third peptide anchor (probably interspaced between the two others) that cannot be detected by fluorescence measurements. Interestingly, the same two-residue-contact principle has recently been found with the class I MHC molecules K^d, K^b, and D^b in sequence analyses of endogenous peptide fractions (Falk et al., 1991). Preliminary sequence results with self peptides eluted from HLA-DR1 and HLA-DR3 do strongly favor our model.

Acknowledgments

We thank Monika Stöhr for excellent technical assistance in performing peptide synthesis and purification and for helpful discussions. We are also grateful to Dr. C. Müller of the Medizin. Klinik Tübingen for providing cell lines WT-100 (BIS) and COX in addition to monoclonal antibodies.

Registry No. Trp, 73-22-3; IM (18–29), 135455-92-4; HA (306–318), 122630-93-7; CS (381–393), 135455-93-5; TUB (3–14), 135455-94-6; TT (763–775), 135455-95-7.

References

Atherton, E., & Sheppard, R. C. (1989) *Solid Phase Peptide Synthesis* (Rickwood, D., & Hames, B. D., Eds.) IRL Press, Oxford.

Benacerraf, B. (1978) *J. Immunol. 120*, 1809–1816.

Berzofsky, J. A., Kurata, A., Takahashi, H., Brett, S. J., & McKean, D. J. (1989) *Cold Spring Harbor Symp. Quant. Biol. 54*, 417–430.

Bjorkman, P., Saper, M. A., Samraoui, B., Bennett, W. S., Strominger, J. L., & Wiley, D. C. (1987) *Nature 329*, 506–512.

Braciale, T. J., Morrison, L. A., Sweetser, M. T., Sambrook, J., Gething, M. J., & Braciale, V. L. (1987) *Immunol. Rev. 98*, 95–121.

Bradford, M. M. (1976) *Anal. Biochem. 72*, 248–254.

Brown, J. H., Jardetzky, T., Saper, M. A., Samraoui, B., Bjorkman, P., & Wiley, D. C. (1988) *Nature 332*, 845–850.

Buus, S., Sette, A., Colon, S. M., Jenis, D. M., G., & Grey, H. M. (1986a) *Cell 47*, 1071–1077.

Buus, S., Sette, A., Colon, S. M., Miles, G., & Grey, H. M. (1986b) *Science 235*, 1353–1366.

Buus, S., Sette, A., Colon, S. M., & Grey, H. M. (1988) *Science 242*, 1045–1049.

Chen, B. P., & Parham, P. (1989) *Nature 337*, 743–746.

Chen, B. P., Madrigal, A., & Parham, P. (1990) *J. Exp. Med. 172*, 779–788.

Chen, G. C., & Young, J. T. (1977) *Anal. Lett. 10*, 1195–1207.

Claverie, J. M., & Kourilsky, P. (1986) *Ann. Inst. Pasteur/Immunol. D137*, 3–21.

Demotz, S., Grey, H. M., Appella, E., & Sette, A. (1989) *Nature 342*, 682–684.

Dornmair, K., & McConnell, H. M. (1990) *Proc. Natl. Acad. Sci. U.S.A. 87*, 4134–4138.

Dornmair, K., Rothenhäusler, B., & McConnell, H. M. (1989) *Cold Spring Harbor Symp. Quant. Biol. 54*, 409–416.

Dornmair, K., Clark, B. R., & McConnell, H. M. (1991) *Proc. Natl. Acad. Sci. U.S.A. 88*, 1335–1338.

Falk, K., Roetzschke, O., Stevanovic, S., Jung, G., & Rammensee, H. G. (1991) *Nature 351*, 290–296.

Fournier, A., Wang, C. T., & Felix, A. M. (1988) *Int. J. Pept. Protein Res. 31*, 86–97.

Garrett, T. P. J., Saper, M. A., Bjorkman, P. J., Strominger, J. L., & Wiley, D. C. (1989) *Nature 342*, 692–696.

Gorga, J. C., Horejsi, V. Johnson, D. R., Raghupathy, R., & Strominger, J. L. (1987) *J. Biol. Chem. 262*, 16087–16094.

Gorga, J. C., Dong, A., Maning, A. D., Woody, R. W., Caughey, W. S., & Strominger, J. L. (1989) *Proc. Natl. Acad. Sci. U.S.A. 86*, 2321–2325.

Greenfield, N., & Fasman, G. D. (1969) *Biochemistry 8*, 4108–4116.

Guillet, J. G., Lai, M. Z., Briner, T. J., Smith, J. A., & Gefter, M. L. (1986) *Nature 324*, 260–263.

Guillet, J. G., Lai, M. Z., Briner, T. J., Buno, S., Sette, A., Grey, H., Smith, J. A., & Gefter, M. L. (1987) *Science 235*, 865–870.

Jardetzky, T. S., Gorga, J. C., Buscg, R., Rothbard, J., Strominger, J. L., & Wiley, D. C. (1990) *EMBO J. 9*, 1797–1803.

Kalbacher, H., & Kropshofer, H. (1991) *J. Chromatogr.* in press.

Kappes, D., & Strominger, J. L. (1988) *Annu. Rev. Biochem. 57*, 991–1028.

Kaufman, J. F., & Strominger, J. L. (1979) *Proc. Natl. Acad. Sci. U.S.A. 76*, 6304–6308.

König, W., & Geiger, R. (1970) *Chem. Ber. 103*, 788–798.

Laemmli, U. K. (1970) *Nature 227*, 680–685.

Lakowicz, J. R. (1987) *Principles of Fluorescence Spectroscopy*, p 264, Plenum Press, New York, London.

Leher, S. S. (1971) *Biochemistry 10*, 3254–3267.

Lotteau, V., Teyton, L., Peleraux, A., Nilsson, T., Karlsson, L., Schmid, S. L., Quaranta, V., & Peterson, P. A. (1990) *Nature 348*, 600–605.

Marrack, P., & Kappler, J. (1988) *Nature 332*, 840–844.

Nikolic-Zugic, J., & Bevan, M. J. (1990) *Nature 344*, 65–68.

Nuchtern, J. G., Biddison, W. E., & Klausner, R. D. (1990) *Nature 343*, 74–76.

Olson, C. A., Williams, L. C., McLaughlin-Tylor, E., & McMillan, M. (1989) *Proc. Natl. Acad. Sci. U.S.A. 86*, 1031–1035.

Peccoud, J., Dellabona, P., Allen, P., Benoist, C., & Mathis, D. (1990) *EMBO J. 9*, 4215–4223.

Reddehase, M. J., & Koszinowski, U. H. (1989) *Nature 337*, 651–653.

Roche, P. A., & Cresswell, P. (1990) *Nature 345*, 615–618.

Roetzschke, O., Falk, K., Deres, K., Schild, H., Norda, M., Metzger, J., Jung, G., & Rammensee, H. G. (1990) *Nature 348*, 252–254.
Rothbard, J. B., & Taylor, W. R. (1988) *EMBO J. 7*, 93–100.
Rothbard, J. B., Lechler, R. I., Howland, K., Bal, V., Eckels, D. D., Sekaly, R., Long, E., Taylor, W. R., & Lamb, J. (1988) *Cell 52*, 515–523.
Rothbard, J. B., Busch, R., Howland, K., Bal, V., Fenton, C., Tylor, W. R., & Lamb, J. (1989) *Int. Immunol. 1*, 479–488.
Sadegh-Nasseri, J., & McConnell, H. M. (1989) *Nature 337*, 274–276.
Saskia de Koster, H., Anderson, D. C., & Termijtelen, A. (1989) *J. Exp. Med. 169*, 1191–1196.
Sinigaglia, F., Guttinger, M., Kilgus, J., Doran, D. M., Matile, H., Etlinger, H., Trzeciak, A., Gillessen, D., & Pink, J. R. L. (1988) *Nature 336*, 778–780.
Stern, O., & Volmer, M. (1918) *Phys. Z. 20*, 183–188.
Sweetser, M. T., Morrison, L. A., Braciale, V. L., & Braciale, T. J. (1989) *Nature 342*, 180–182.
Townsend, A. R. M., Gotch, F. M., & Davey, J. (1985) *Cell 42*, 457–461.
Townsend, A. R. M., Rothbard, J., Gotch, F. M., Pahadur, G., Wraith, D., & McMichael, A. J. (1986) *Cell 44*, 959–967.
Van Bleek, G., & Nathenson, S. G. (1990) *Nature 348*, 213–216.
Viguier, M., Dornmair, K., Clark, B. R., & McConnell, H. (1990) *Proc. Natl. Acad. Sci. U.S.A.* 7170–7174.
Wallny, H. J., & Rammensee, H. G. (1990) *Nature 343*, 275–278.
Ziegler, K., & Unanue, E. R. (1982) *Proc. Natl. Acad. Sci. U.S.A. 79*, 175–192.

Solution Conformational Preferences of Immunogenic Peptides Derived from the Principal Neutralizing Determinant of the HIV-1 Envelope Glycoprotein gp120†

K. Chandrasekhar,‡ Albert T. Profy,§ and H. Jane Dyson*,‡
Department of Molecular Biology, Research Institute of Scripps Clinic, La Jolla, California 92037, and Repligen Corporation, Cambridge, Massachusetts 02139

Received May 14, 1991; Revised Manuscript Received July 3, 1991

ABSTRACT: With standard one- and two-dimensional proton NMR techniques, a common structural motif has been identified in water solutions of short peptide sequences derived from the envelope glycoprotein gp120 of HIV-1. Three peptides of lengths 12, 24, and 40 residues (termed RP342, RP142, and RP70, respectively) were synthesized, each containing a central amino acid sequence common to many HIV-1 isolates. In addition, RP70 contained a disulfide bond between cysteine residues close to the ends of the molecule, forming a loop that is thought to constitute an important structural and immunological component of the intact glycoprotein. Peptides RP70 and RP142 showed evidence for the presence of a significant population of conformations containing a β-turn in the conserved sequence Gly-Pro-Gly-Arg. Strong nuclear Overhauser effect (NOE) connectivities were observed between the amide protons of the arginine and the adjacent glycine. A weak NOE connectivity was observed between the $C^{\alpha}H$ of the proline residue and the NH of the Arg [a $d_{\alpha N}(i,i+2)$ NOE connectivity], confirming the presence of a conformational preference for a turn conformation in this sequence. The remainder of the peptide showed evidence of conformational averaging: no NMR evidence for a uniquely folded structure was obtained for any of the peptides in water solution. Circular dichroism (CD) spectra indicated that no ordered helix was present in water solutions of RP70, although a CD spectrum that indicated the presence of approximately 30% helix could be induced by the addition of trifluoroethanol. Changes are observed in the NMR spectrum of RP70 in TFE/water mixtures consistent with helix formation, and the β-turn is apparently retained.

Several candidate vaccines designed to provide protection from human immunodeficiency virus type 1 (HIV-1) infection are based on the viral envelope glycoprotein gp160 and its derivatives gp120 and gp41 (Bolognesi, 1989). Although several sites on these proteins have been reported to be targets for neutralizing antibodies, it is now clear that the principal neutralizing determinant (PND)[1] is located within a disulfide-linked loop in the V3 region of gp120 (Rusche et al., 1988; Palker et al., 1988; Javaherian et al., 1989). Due to sequence variability in this region, antisera raised against the PND of one isolate generally do not neutralize other isolates (Matthews et al., 1986; Putney et al., 1986; Goudsmit et al., 1987; Rusche et al., 1988), and this type specificity has been an obstacle for vaccine development. Analysis of 245 PND sequences, however, revealed that certain amino acid residues are relatively conserved (LaRosa et al., 1990). The sequence Gly-Pro-Gly-Arg, in particular, was present in 84% of the PNDs studied, and significantly, antisera directed against the slightly longer sequence Gly-Pro-Gly-Arg-Ala-Phe were shown to neutralize multiple isolates (Javaherian et al., 1990). The

† This research was supported in part by Grant CA 27498 from the National Institutes of Health. K.C. was supported by a fellowship from the Repligen Corp.
‡ Research Institute of Scripps Clinic.
§ Repligen Corporation.

[1] Abbreviations: NMR, nuclear magnetic resonance; CD, circular dichroism; 2QF-COSY, double-quantum filtered two-dimensional correlated spectroscopy; NOESY, two-dimensional nuclear Overhauser effect spectroscopy; R-COSY, relayed-COSY spectroscopy; PND, principal neutralizing determinant.

0006-2960/91/0430-9187$02.50/0